Functional Coupling of Ca^{2+} Channels to Ryanodine Receptors at Presynaptic Terminals

Amplification of Exocytosis and Plasticity

K. Narita,* T. Akita,‡ J. Hachisuka,‡ S.-M. Huang,‡ K. Ochi,* and K. Kuba‡

From the *Department of Physiology, Kawasaki Medical School, Kurashiki 701-0192, Japan; and ‡Department of Physiology, School of Medicine, Nagoya University, Nagoya 466-8550, Japan

abstract Ca^{2+}-induced Ca^{2+} release (CICR) enhances a variety of cellular Ca^{2+} signaling and functions. How CICR affects impulse-evoked transmitter release is unknown. At frog motor nerve terminals, repetitive Ca^{2+} entries slowly prime and subsequently activate the mechanism of CICR via ryanodine receptors and asynchronous exocytosis of transmitters. Further Ca^{2+} entry inactivates the CICR mechanism and the absence of Ca^{2+} entry for >1 min results in its slow depriming. We now report here that the activation of this unique CICR markedly enhances impulse-evoked exocytosis of transmitter. The conditioning nerve stimulation (10–20 Hz, 2–10 min) that primes the CICR mechanism produced the marked enhancement of the amplitude and quantal content of end-plate potentials (EPPs) that decayed double exponentially with time constants of 1.85 and 10 min. The enhancement was blocked by inhibitors of ryanodine receptors and was accompanied by a slight prolongation of the peak times of EPP and the end-plate currents estimated from deconvolution of EPP. The conditioning nerve stimulation also enhanced single impulse- and tetanus-induced rises in intracellular Ca^{2+} in the terminals with little change in time course. There was no change in the rate of growth of the amplitudes of EPPs in a short train after the conditioning stimulation. On the other hand, the augmentation and potentiation of EPP were enhanced, and then decreased in parallel with changes in intraterminal Ca^{2+} during repetition of tetani. The results suggest that ryanodine receptors exist close to voltage-gated Ca^{2+} channels in the presynaptic terminals and amplify the impulse-evoked exocytosis and its plasticity via CICR after Ca^{2+}-dependent priming.

key words: Ca^{2+}-induced Ca^{2+} release • Ca^{2+}-dependent priming • transmitter release • end-plate potential • frog motor nerve terminals

INTRODUCTION

A nerve impulse triggers exocytosis of neurotransmitter via Ca^{2+} entry through voltage-dependent Ca^{2+} channels at the presynaptic terminals (see Katz, 1969). A large increase in cytoplasmic free Ca^{2+} concentration ($[Ca^{2+}]_i$) close to the internal orifice of the Ca^{2+} channel (Ca^{2+} microdomain) is thought to activate low affinity Ca^{2+} receptors of exocytotic machinery (Llinás et al., 1992; Heidelberger et al., 1994; Schweitzer et al., 1995). A global rise in $[Ca^{2+}]_i$ in the terminal produced by repetitive nerve activity as well as a rise in the Ca^{2+} microdomain also regulates the efficacy of impulse-induced exocytosis of neurotransmitter, presumably via high affinity Ca^{2+} receptors (Kamiya and Zucker, 1994; Zucker, 1996). These Ca^{2+} actions on transmitter release processes should be enhanced, if intracellular Ca^{2+} release occurs in response to Ca^{2+} entry, similar to the cell soma and dendrites of neurons (Kuba, 1980; Friel and Tsien, 1992; Hua et al., 1993; Llano et al., 1994; Garaschuk et al., 1997; for review, see Kuba, 1994). There is little direct evidence, however, for the involvement of Ca^{2+} entry-induced Ca^{2+} release in the impulse-evoked exocytosis of transmitter (Onodera, 1973; Smith and Cunnane, 1996; Mothét et al., 1998).

Previously, we reported a unique Ca^{2+}-induced Ca^{2+} release (CICR)[1] mechanism via ryanodine receptors at frog motor nerve terminals. Ca^{2+} entry produced by repetitive nerve activity primes the mechanism of CICR for activation over a few minutes, and then activates CICR, enhancing the asynchronous release of transmitter. This CICR mechanism is inactivated by further Ca^{2+} entry, and restored by a short pause of Ca^{2+} entry, but falls in a deprimed state after a long absence of Ca^{2+} entry (Narita et al., 1998). We now report here that Ca^{2+} release via this mechanism is closely coupled with Ca^{2+} entry through voltage-dependent Ca^{2+} channels and amplifies the impulse-induced rise in $[Ca^{2+}]_i$, enhancing neurotransmitter exocytosis and the longer modes of its short term plasticity, "augmentation" and "potentiation." This novel role of CICR in the amplifi-

Dr. Akita and Mr. Hachisuka contributed equally to this paper.

Address correspondence to Dr. Kenji Kuba, Department of Physiology, School of Medicine, Nagoya University, 65 Tsurumai-cho, Showa-ku, Nagoya 466-8550, Japan. Fax: 81-52-744-2049; E-mail: kubak@med.nagoya-u.ac.jp

[1]*Abbreviations used in this paper:* CICR, Ca^{2+}-induced Ca^{2+} release; EPC, end-plate current; EPP, end-plate potential; MEPP, miniature EPP; QC, quantal content.

 J. Gen. Physiol. © The Rockefeller University Press • 0022-1295/2000/04/519/14 $5.00
Volume 115 April 2000 519–532
http://www.jgp.org/cgi/content/full/115/4/519

cation of exocytosis would provide an important basis in general for the mechanism of synaptic plasticity.

MATERIALS AND METHODS

Preparations and experimental procedures are essentially similar to those of the previous study (Narita et al., 1998). Cutaneus pectoris or sartorius muscles of frogs (*Rana nigromaculata*) were isolated with the innervating nerve. There was no difference in the results obtained from these two types of muscle. The composition of normal Ringer's solution (mM) was: 100 NaCl, 2 KCl, 2.5 $CaCl_2$, 3.0 $MgCl_2$, 8.0 Tris, pH 7.4, or 111 NaCl, 2 KCl, 1.8 $CaCl_2$, 5.0 HEPES-Na, pH 7.4, 5.0 glucose. There was no significant difference in the data obtained from the preparation isolated in different types of Ringer's solution. A conventional intracellular recording technique was applied to record end-plate potentials (EPPs) using electrodes filled with 3 M KCl at 20–24°C. Low Ca^{2+}, high Mg^{2+} solutions were made by lowering $CaCl_2$ (0.02–0.5 mM) and adding $MgCl_2$ (10 mM) with the adjustment of osmolarity by changing NaCl concentration. The quantal content (QC) of EPP was calculated by dividing the mean amplitude of EPP by the mean amplitude of miniature EPPs (MEPPs) recorded under the same condition. The time course of end-plate current (EPC) was calculated by the deconvolution of that of EPP (digitized at 50 kHz). The Fourier transform of EPP was taken and divided by the Fourier transform of the cable equation (the membrane time constant, 20 ms) for the impulse response (Fatt and Katz, 1951; Gage and McBurney, 1973). The inverse Fourier transform of the result of division yielded the time course of EPC. The rising phase of the calculated EPC would reliably reflect that of the EPC recorded by voltage clamping the end-plate membrane for two reasons. First, the applicability of the cable equation to the muscle end-plate membrane has been well established (Fatt and Katz, 1951; see review by Gage, 1976). Second, the time course of the EPC calculated from an EPP was nicely fit to that of the EPC recorded under the voltage-clamp condition (Takeuchi and Takeuchi, 1959; see Gage, 1976).

Changes in $[Ca^{2+}]_i$ in motor nerve terminals were measured from those of frog (*Rana nigromaculata*) cutaneus pectoris muscles separately from the experiments recording EPPs. The composition of normal Ringer's solution (mM) was: 112 NaCl, 2 KCl, 1.8 $CaCl_2$, 2.4 $NaHCO_3$, pH 7.4, when equilibrated with air, with or without glucose 5.0, or the Ringer's solution buffered with HEPES used for recording EPPs (see above). There was no significant difference between the characteristics of the impulse-induced Ca^{2+} dynamics and CICR recorded in different types of Ringer's solution. Low Ca^{2+}, high Mg^{2+} solutions were similar to those for recording EPPs. K-salt of dextran-conjugated Oregon green BAPTA-1 (d-OGB-1: mol wt 10,000) was loaded into the terminals as described previously (Narita et al., 1998). This high-affinity Ca^{2+} indicator yielded the excellent signal to noise ratio (S/N ratio) of an impulse-induced rise in $[Ca^{2+}]_i$ in frog motor nerve terminals. Although we tried to use a low-affinity Ca^{2+} indicator, OGB-5N, which would be apparently suited for recording high $[Ca^{2+}]_i$ in the microdomain for exocytosis at a faster rate, we were unable to record reliably impulse-induced rises in $[Ca^{2+}]_i$ at a high S/N ratio with this indicator because of its weak fluorescence before stimulation. In most experiments, a confocal laser scanning unit (MRC-600; Nippon Biorad) with a Kripton-Argon laser (488 nm) in combination with an inverted microscope (TMD-300; objective, Nikon 40× water/N.A. 1.15; Nikon, Inc.) was used to measure fluorescence changes of d-OGB-1. Fluorescence images were taken by a line-scanning mode at 500 Hz. In some experiments, fluorescence was measured with a cooled CCD-camera (Argus/HiSca, C6790-81; Hamamatsu Phototonics) through an image intensifier attached to an upright microscope (Zeiss Axioscope, objective 60× water/N.A. 0.95; Karl Zeiss Japan) and analyzed by image analysis software (Argus; Hamamatsu Phototonics). In the analyses of fluorescence images of d-OGB-1, the ratios of the images during and after nerve stimulation to that before stimulation were taken and analyzed as in previous experiments (Narita et al., 1998). For conversion of fluorescence intensity ratio to $[Ca^{2+}]_i$, the K_d of d-OGB-1 were assumed to be 500 nM and the ratio of the maximum to the minimum fluorescence was 15.0. The basal $[Ca^{2+}]_i$ was assumed to be 10–70 nM for the following reasons. When we used the previous value of 72 nM in conversion of some data, the $[Ca^{2+}]_i$ value calculated from an increase in fluorescence ratio induced by a single stimulus progressively elevated during a short train under the control condition. We thought that this progressive increase during such a short train was unrealistic, since constant increases in single impulse-induced rise in $[Ca^{2+}]_i$ were seen in other experiments such as those at the beginning of a tetanus shown in Fig. 7 C (in which the basal $[Ca^{2+}]_i$ was assumed to be 70 nM) and also in other motor nerve terminals (DiGregorio and Vergara, 1997; David et al., 1997). Accordingly, we presumed that the apparent, progressive increase in impulse-induced Ca^{2+} responses seen in some experiments resulted from the incorrect assumption of the basal $[Ca^{2+}]_i$ value, which would have been higher than the real one in those terminals.

d-OGB-1 was obtained from Molecular Probes, Inc. TMB-8 [8-(*N*,*N*-diethylamino)octyl3,4,5-trimethoxybenzoate hydrochloride] was from Sigma Chemical Co. or Tokyo Kasei Kogyo Co. Ryanodine and HEPES-Na or -K, were from Sigma Chemical Co.

RESULTS

Enhancement of Impulse-induced Transmitter Release by CICR

EPPs were intracellularly recorded in a low Ca^{2+}, high Mg^{2+} solution. A short train of 20 stimuli at 50 Hz to the nerve was repeated 10–20× every 20 s in a low Ca^{2+}, high Mg^{2+} solution (Fig. 1 A). The averages for the amplitudes of individual EPPs in trains were taken and divided by MEPPs, yielding QC of EPP (see Fig. 3 A; ● and ×). The amplitude and QC increased during a short train of stimuli, indicating the facilitation of evoked release of transmitter (Zengel and Magleby, 1982).

To observe how CICR affects impulse-induced exocytosis, the nerve was stimulated by a relatively long tetanus at a moderate frequency (10 Hz) for 10 min, which is expected to fully prime the mechanism of CICR (Narita et al., 1998). EPPs slowly and then progressively increased in amplitude during the tetanus, while its failure and variability decreased (Fig. 1, C and D). [When the tetanus was further continued for more than 10 min, the EPP amplitude reached the maximum, and then declined toward the level before the tetanus (not shown) due to the inactivation of CICR, as seen in a MEPP-hump (Narita et al., 1998).]

After this conditioning tetanus, the amplitude and QC of the first EPPs in a short train of 20 stimuli at 50 Hz were markedly enhanced 15.6× (±2.7, SEM, $n = 16$ for both) those before the conditioning tetanus (0.11 ± 0.02 mV, 0.24 ± 0.05, respectively; Figs. 1 B and 3 A, ○). This enhancement of the first EPP in a short train must be caused by potentiation of transmitter release and the activation of CICR (see below), but not other forms of

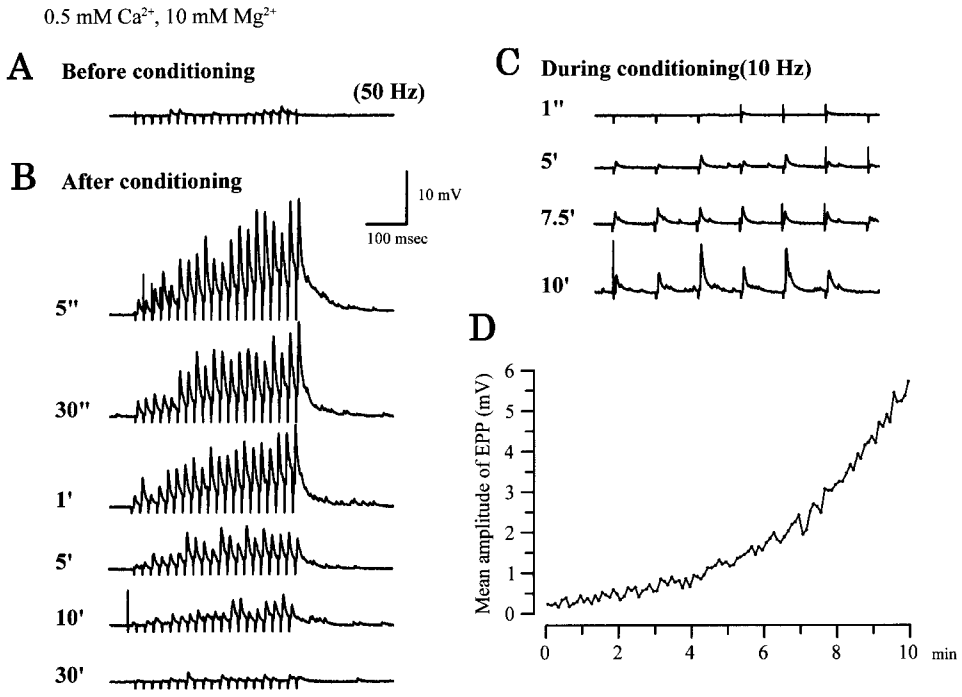

Figure 1. Enhancement of EPPs by a conditioning tetanus that primes the mechanism of CICR at the nerve terminal. (A) A train of EPPs induced by 20 stimuli at 50 Hz before a conditioning tetanus (10 Hz, 10 min) in a low Ca^{2+} (0.5 mM), high Mg^{2+} (10 mM) solution. (B) Trains of EPPs (20 stimuli, 50 Hz) induced at variable times after the conditioning tetanus. (C) Changes in EPPs during the conditioning tetanus. Sample records are those at 1 s, and 5, 7.5, and 10 min after the beginning of the tetanus. (D) The time course of changes in EPP amplitude during the conditioning tetanus. Each point represents the mean of 60 EPPs recorded for a period of 6 s.

short-term plasticity, facilitation, and augmentation, because this relatively short-lasting plasticity should have disappeared within a 10-s interval. The decay time course of the enhancement of transmitter release produced by a conditioning tetanus was examined by applying a train of 20 stimuli (50 Hz) every 10 s after the end of the tetanus. The enhancement of the amplitude of the last EPP in a train decayed double exponentially with time constants of 1.85 (±0.15, $n = 5$: the fraction of amplitude, 48.9 ± 9.2%) and 10.4 (±1.0) min (see Fig. 4 A). The initial component of the enhancement can be explained by potentiation, the longest form of short-term plasticity, since its time constant falls within that of potentiation (Magleby and Zengel, 1975). (It may be noted that the enhancement of the last EPP in a short train was multiplied by facilitation, but not by augmentation for the trains given every 10 s.) The time constant of the later component is similar to that of the depriming process of CICR (Narita et al., 1998).

The enhancement of EPP by a conditioning tetanus was strongly inhibited after treatment with blockers of ryanodine receptors, ryanodine (20 μM: Figs. 2 B and 3 B, ○ and ●) and TMB-8 (8 μM: Chiou and Malagodi, 1975; not shown). The amplitude and QC of the first EPP in a short train after a conditioning tetanus (10 Hz, 10 min) was 3.2× (±1.7, $n = 9$ for both) those before the tetanus (0.10 ± 0.04 mV, 0.22 ± 0.08, respectively) in the presence of ryanodine. The amplitude of the last EPP in a short train after the conditioning tetanus (1.02 ± 0.32 mV, $n = 6$) decayed single exponentially in three cells with time constants (12.8, 15.8, and 3.8 min) or remained unchanged in other cells (Fig. 4 B). This indicates that potentiation as well as the activation of CICR disappeared or decreased markedly in the presence of ryanodine. The slow growth of EPP amplitude during the conditioning tetanus did not continue and changed to a decline before the end of tetanus in the presence of ryanodine (20 μM), indicating that the blockade of ryanodine receptor depends on its activation (Fig. 2, C and D).

CICR Does Not Affect Facilitation of Transmitter Release

The rate of growth of QC of EPPs induced by a short train of stimuli remained unchanged after a long conditioning tetanus that primed the mechanism of CICR (Fig. 3 A; × and ○). The rate of growth of QC of EPPs by a short train was also unchanged by the conditioning tetanus in the presence of ryanodine (Fig. 3 B; × and ∗). These results indicate that facilitation, presumably the fast component (Zengel and Magleby, 1982; Zucker, 1996; the fast component comprises ~80%, Tanabe and Kijima, 1992), was not affected by the activation of CICR, although it markedly enhanced transmitter release.

Enhancement of Repetitive Impulse-induced Rises in $[Ca^{2+}]_i$ by CICR

We examined how the rise in $[Ca^{2+}]_i$ in the motor nerve terminal induced by a short train changes after a conditioning tetanus that primes the mechanism of CICR. Rises in $[Ca^{2+}]_i$ induced by a short train of stimuli (~20–30 stimuli, 50 Hz) were recorded by measuring fluorescence changes of OGB-1 loaded in the mo-

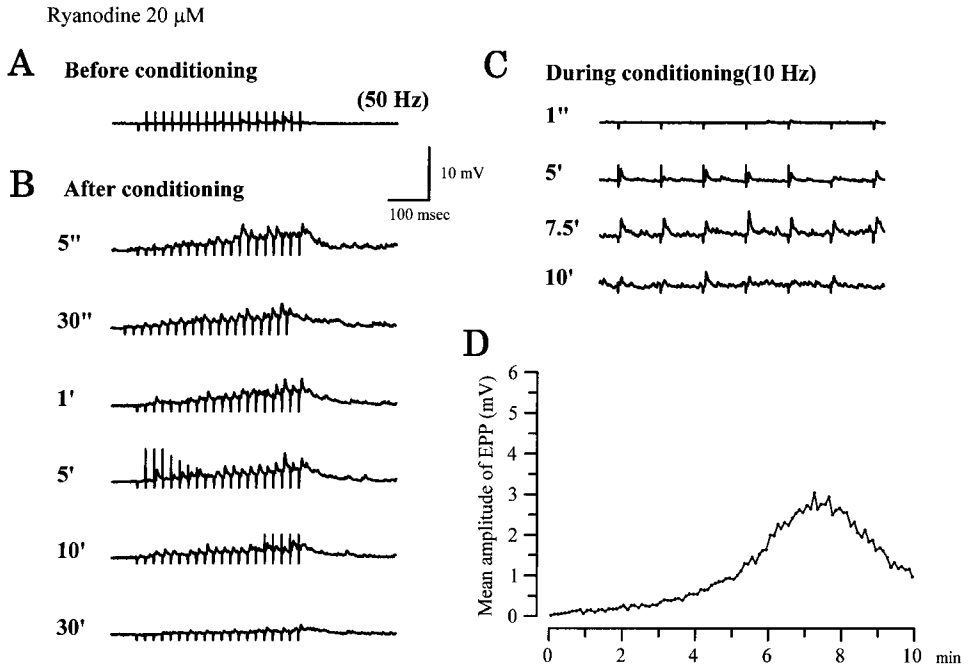

Figure 2. Effects of ryanodine on EPPs during a conditioning tetanus and the enhancement of the amplitudes of EPPs produced by the conditioning tetanus. All the records were taken after superfusion with a low Ca^{2+} (0.5 mM), high Mg^{2+} (10 mM) solution containing ryanodine (20 μM) for 60 min. Explanations are identical for those in Fig. 1.

tor nerve terminals in a low Ca^{2+} and high Mg^{2+} (Ca^{2+}/Mg^{2+} > 0.2 mM/10 mM) solution with a cooled CCD camera. Changes in the ratio of the fluorescence intensity during and after a short train of stimuli to that before the train were converted to those in $[Ca^{2+}]_i$ (Fig. 5 A). A conditioning tetanus (10 Hz, 6 min) caused the marked enhancement of short train-induced rises in $[Ca^{2+}]_i$ (to 180 ± 17% at 15–50 s after the tetanus; the control amplitude, 44.9 ± 5.6 nM, n = 7), which lasted for more than 16 min (Fig. 5 A, a). This enhancement was completely blocked by ryanodine (10 μM) applied for 30 min (n = 5; Fig. 5 A, b). Similar enhancements were also seen in normal Ringer's solution (Fig. 5 B; to 166 ± 25% at 10–45 s; the control amplitude, 93.0 ± 11.2 nM, n = 4).

To observe further how the increase in $[Ca^{2+}]_i$ induced by each impulse in a short train is affected by a conditioning tetanus that primes CICR, line scanning was made to motor nerve terminals loaded with dOGB-1 (Fig. 6, A and B) in normal Ringer's solution, in

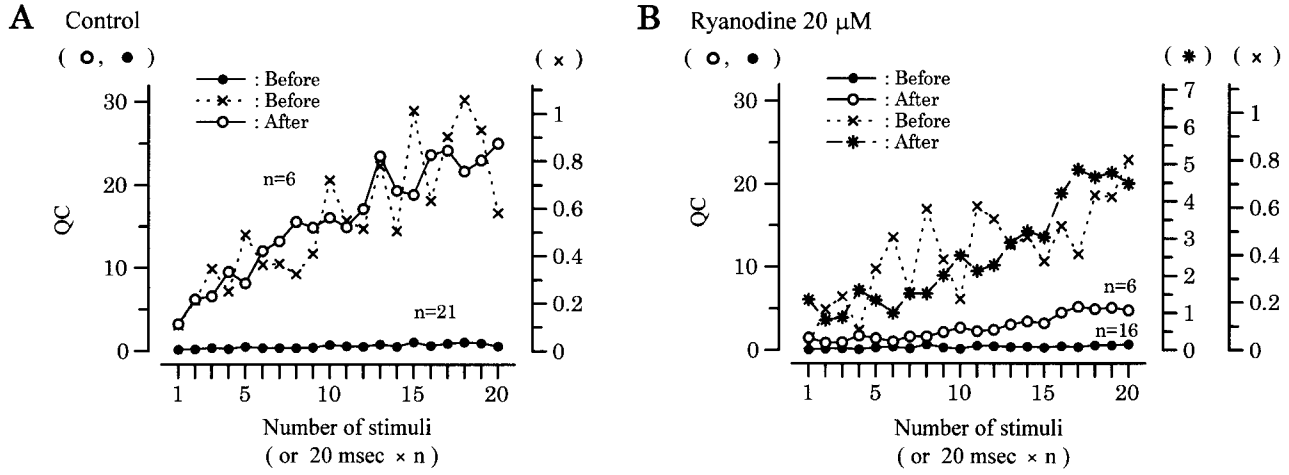

Figure 3. The rates of growth of QC of EPPs during a short train before and after a conditioning tetanus. All data were obtained from the experiments shown in Figs. 1 and 2. (A and B) The rate of increases in QC of each of 20 EPPs (50 Hz) before and after the conditioning tetanus (10 Hz, 10 min). (● and ○) QCs of EPPs before and after the conditioning tetanus, respectively, in the absence (A) and presence (B) of ryanodine (20 μM). (× and *) QCs of EPPs before (×) and after (*, only for those in B) the conditioning tetanus replotted in enlarged scales of the right ordinates to compare their relative changes during a short train. Each symbol represents the QC of n^{th} averaged EPP in each train (the number of trains is shown in the graphs), which was calculated by dividing the mean of EPPs by the mean amplitude of miniature EPPs.

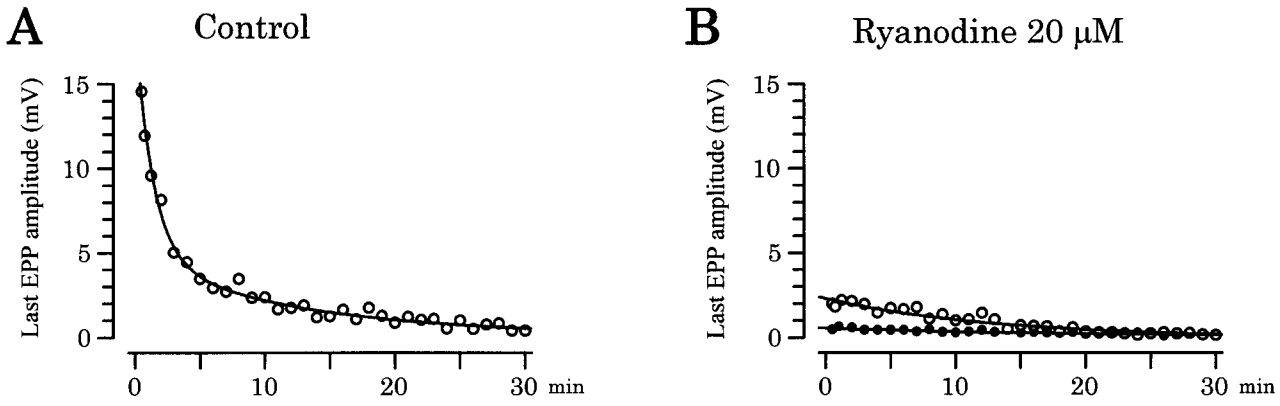

Figure 4. The decay time course of the enhancement of EPP amplitude after the conditioning tetanus in the absence and presence of ryanodine. (A) The decay time courses of the enhanced EPP in a train after the conditioning tetanus (10 Hz, 10 min). The averaged amplitudes of the last EPPs in trains recorded after the conditioning tetanus were plotted against the time after the end of tetanus. The time course was fitted by the equation, EPP = $9.5\exp(-t/1.4) + 4.5\exp(-t/12.0)$ (mV/min). (B) The decay time courses of the enhanced EPPs in a train after the conditioning tetanus in the presence of ryanodine (20 μM). (○) The decay of EPPs recorded after the first conditioning tetanus at 30 min after the application of ryanodine; (●) the decay of EPPs after the second tetanus applied at 130 min. The time courses shown by ○ and ● were fitted by the equations, EPP = $2.24\exp(-t/12.8)$ and EPP = $0.44\exp(-t/15.9)$, respectively.

which individual rises in $[Ca^{2+}]_i$ evoked by each impulse were discerned. Changes in the ratio of the fluorescence intensity during and after a short tetanus to that before the tetanus were converted to those of $[Ca^{2+}]_i$, and then plotted against time (Fig. 6 C). Each stimulus during a short train of 20 stimuli (50 Hz) produced rises in $[Ca^{2+}]_i$ in the motor nerve terminal, which progressively increased in decay rate and summed up to a plateau within 10–15 stimuli for matching of individual decay rates with the stimulation

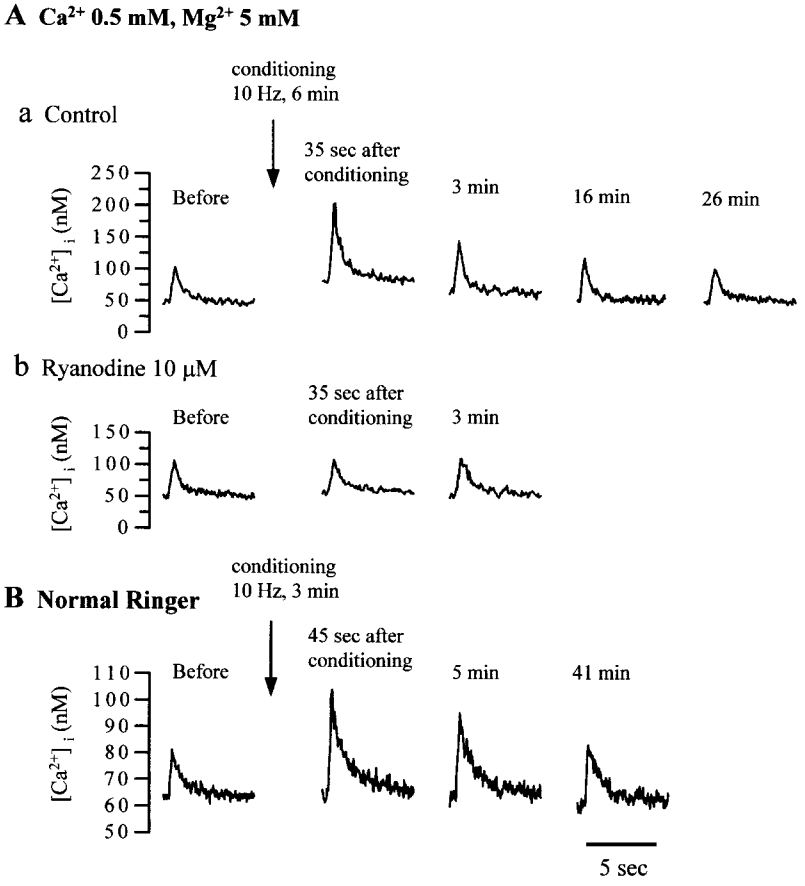

Figure 5. Enhancement of a test tetanus-induced rise in $[Ca^{2+}]_i$ after the conditioning tetanus and the blockade by ryanodine. (A) Enhancement of a test tetanus-induced rise in $[Ca^{2+}]_i$ (50 Hz, 20 pulses) after the conditioning tetanus (10 Hz, 6 min) and its blockade by ryanodine (10 μM) in a low Ca^{2+}, high Mg^{2+} solution. Ryanodine was applied for 30 min. (B) Enhancement of a test tetanus-induced rise in $[Ca^{2+}]_i$ (50 Hz, 10 pulses) after the conditioning tetanus (10 Hz, 3 min) in normal Ringer solution. Test tetanus-induced rises in $[Ca^{2+}]_i$ were recorded by measuring changes in dOGB-1 fluorescence with an intensified CCD camera.

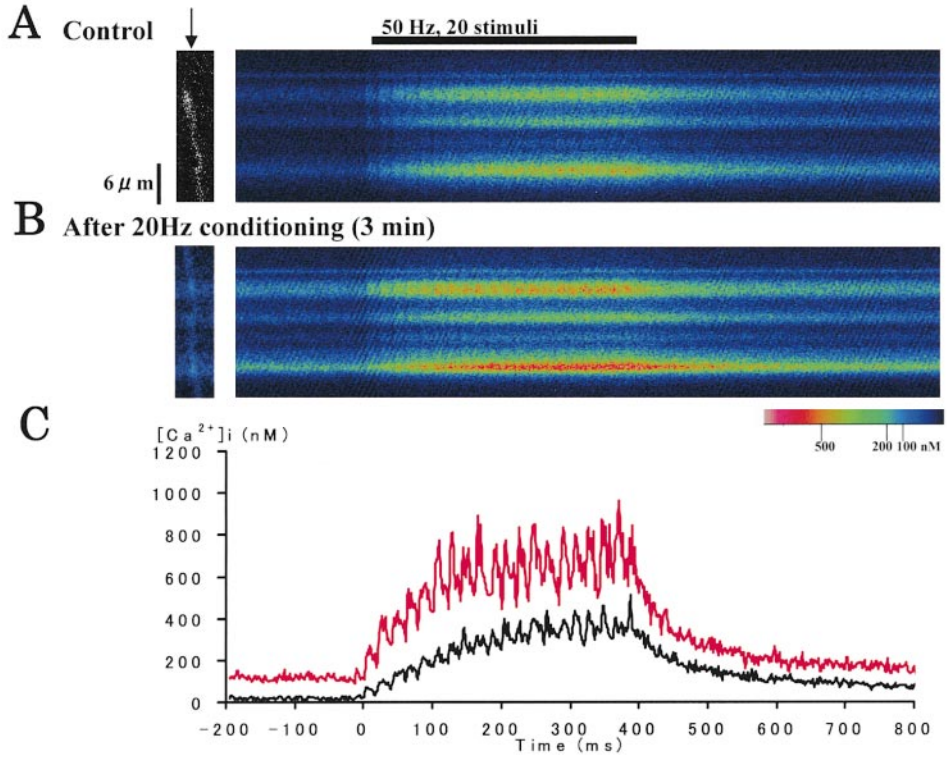

Figure 6. Enhancement of tetanus-induced rises in $[Ca^{2+}]_i$ in the nerve terminal after the priming of CICR by a conditioning tetanus. (A and B) Increases in $[Ca^{2+}]_i$ in the nerve terminal induced by a train of 20 stimuli at 50 Hz (test tetanus) before and after the conditioning tetanus (20 Hz, 3 min). Fluorescent images (right) were obtained by line scanning the nerve terminal loaded with dOGB-1 along the long axis of the nerve terminal with a confocal microscope in normal Ringer (20 images were averaged). Small images in the left side are X-Y scanned images before stimulation, which are superimposed by a part of the line-scanned image to show the scanned line. The ratio of fluorescence intensity at each line to those before a train of stimuli applied in a period before the conditioning tetanus was taken. The time bases in A and B correspond to that of the graph in C. (C) The time course of increases in $[Ca^{2+}]_i$ before, during, and after a test tetanus applied before or after the conditioning tetanus. Black and red lines are changes in $[Ca^{2+}]_i$ before and after the conditioning tetanus, respectively.

interval (Fig. 6 C). The magnitude of the first response in a train was 47.9 ± 4.4 nM (n = 5). The peak of the last response measured from the prestimulation level was 363 ± 42 nM (n = 5). The decay phase of $[Ca^{2+}]_i$ after the end of a train followed a double exponential function with time constants, 48 ± 10 ms (59 ± 6% in amplitude) and 410 ± 107 ms (n = 5).

After the application of a conditioning tetanus (20 Hz, 3 min; see changes in $[Ca^{2+}]_i$ produced by a similar tetanus in Fig. 7 C), a rise in $[Ca^{2+}]_i$ induced by each stimulus of a short train (50 Hz, 20 pulses) was amplified (Fig. 6, B and C; 77 ± 19 nM, n = 5, averaged over the first responses in a short train recorded for 15 s to 3 min). The magnitude of the last responses in a train was 475 ± 68 nM (n = 5), and decayed double exponentially with the time constants (51 ± 8 and 305 ± 43 ms, n = 5; fast component, 52 ± 5%) that were slightly smaller than those before the conditioning tetanus. This amplification in tetanus-induced rises in $[Ca^{2+}]_i$ by the conditioning tetanus decayed over a few minutes to >10 min (not shown, but see Fig. 5 B for similar experiments).

The long conditioning tetanus thus primes and activates the mechanism of CICR in frog motor nerve terminals (Narita et al., 1998), causing the slow growth of EPP. Once the mechanism of CICR is primed, Ca^{2+} entry induced by a single nerve impulse markedly enhances neurotransmitter release. Two possible mechanisms may explain the enhancement. First, CICR may amplify the rise in $[Ca^{2+}]_i$ in Ca^{2+} microdomains close to exocytotic machinery so that CICR is directly involved in the impulse-evoked exocytosis. This mechanism may be reflected in the late slow decay phase of the enhanced EPP after the conditioning tetanus (Fig. 4 A). Second, CICR may enhance Ca^{2+}-dependent short-term plasticity of transmitter release, which consists of fast and slow types of facilitation (time constants; 30–60 and 400 ms, respectively), augmentation (7 s) and potentiation (several minutes; Katz and Miledi, 1968; Magleby and Zengel, 1975; Zengel and Magleby, 1982; Delaney and Tank, 1994; Regehr et al., 1994; Zucker, 1996). Among them, facilitation (presumably fast type) was already shown to be unaffected by the activation of CICR.

Effects of CICR on the Time Courses of Single Impulse-induced Rises in $[Ca^{2+}]_i$, EPP, and End-Plate Current

If the site of CICR is remote from that of Ca^{2+} entry, CICR should occur with a time delay after Ca^{2+} entry, and be reflected in the time course of an impulse-induced rise in $[Ca^{2+}]_i$ (see discussion). For instance, if the time delay for Ca^{2+} release after Ca^{2+} entry is long enough, the diphasic time course of an impulse-induced rise in $[Ca^{2+}]_i$ may be recorded as seen in synaptically

evoked Ca^{2+} transients in the cerebellar Purkinje neurons, in which not only Ca^{2+} entry, but also inositoltrisphophate-induced Ca^{2+} release are involved (Finch and Augustine, 1998; Takechi et al., 1998). On the other hand, if the time difference between the onsets of Ca^{2+} entry and Ca^{2+} release was short enough, a single phasic rise in $[Ca^{2+}]_i$ would be seen (see discussion).

We recorded the whole time course of single impulse-induced rise in $[Ca^{2+}]_i$ before and after a conditioning tetanus (10 Hz, 5 min) in normal Ringer. An increase in $[Ca^{2+}]_i$ produced by a single stimulus rose in 5 ms (5.7 ± 0.9 ms, $n = 6$, 10–90% rise time) to the peak (44.7 ± 2.9 nM, $n = 6$) and decayed double exponentially (τ_1, 46 ± 6 ms, 79.6 ± 6.4%; τ_2, 282 ± 70 ms, $n = 6$; see Fig. 7, A and B). When a conditioning tetanus of 10 Hz for 3–10 min was given to the nerve, a rise in $[Ca^{2+}]_i$ induced by individual stimuli slowly increased throughout the course of the tetanus (Fig. 7 C) with the elevation of the basal level by 82 ± 18 nM ($n = 5$), which decayed with the time constant of 1.65 ± 0.4 min ($n = 6$: Fig. 7 D). After the conditioning tetanus, impulse-induced rises in $[Ca^{2+}]_i$ were markedly enhanced in amplitude (to 3.1 ± 0.7 × the control, $n = 7$; averaged over those for a period of 5–35 s) and rate of rise (to 3.1 ± 0.8×, $n = 6$; Fig. 7, A and B). The enhancement decayed over a few minutes to 10 min after the conditioning tetanus (Fig. 7 A). During the enhancement, the peak time was not changed (Fig. 7 B: 105 ± 17% of that before the tetanus, $n = 6$) and the time constants of the double exponential decay were slightly decreased (τ_1, 88 ± 16%; τ_2, 79 ± 18%, $n = 6$) with no change in their fraction (fast component; 70.8 ± 3.9%, $n = 6$). The enhancement of single impulse-induced rise in $[Ca^{2+}]_i$ after the conditioning tetanus was not seen in the presence of thapsigargin applied for 30–90 min (92 ± 11%, $n = 4$; the magnitude of rise before the conditioning tetanus was 67.8 ± 17.2 nM). Pharmacological priming of the CICR mechanism by caffeine (2 mM) also enhanced single impulse-induced increases in $[Ca^{2+}]_i$ (to 160 ± 20%, $n = 5$; control, 40.3 ± 0.3 nM) with no change in peak time (94 ± 3%; control, 4.1 ± 0.6 ms; Fig. 8, A and B). Thus, the activation of CICR does not apparently prolong the time course of a single impulse-induced rise in $[Ca^{2+}]_i$, but markedly enhances its amplitude.

The more straightforward way of testing the involvement of CICR in the Ca^{2+} microdomain for impulse-induced exocytosis would be to examine the time course of transmitter release induced by a nerve impulse. Changes in the time course of transmitter release may be reflected in the rising phase of the EPC underlying an EPP. The peak times of EPP (1.71 ± 0.08 ms, $n = 5$) and EPC (see materials and methods for estimation: 596 ± 47 μs) were increased by 227 μs (±69 μs; Fig. 9 A) and 200 μs (±65 μs; Fig. 9 B), respectively, after the conditioning tetanic stimulation (10 Hz, 10 min) that increased their amplitude markedly. This indicates that the time course of transmitter release is prolonged when CICR is activated in response to Ca^{2+} entry. This implies that the conditioning tetanus recruited a new impulse-induced source of Ca^{2+}.

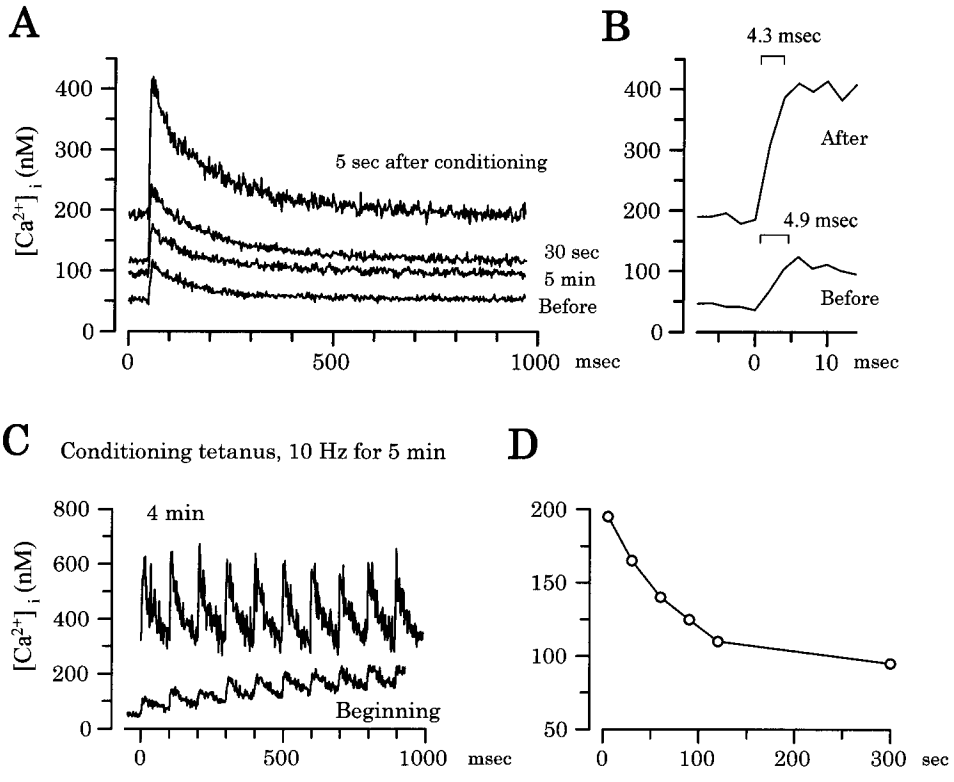

Figure 7. Enhancement of single impulse-induced rises in $[Ca^{2+}]_i$ by a conditioning tetanus. (A) Single impulse-induced rises in $[Ca^{2+}]_i$ before and 5 s, 30 s, and 5 min after a conditioning tetanus (10 Hz, 5 min). Single impulse-induced rises in $[Ca^{2+}]_i$ were recorded by line-scanning the terminal loaded with dOGB-1 with a confocal microscope in normal Ringer, and changes in the fluorescence of dOGB-1 were averaged over 3–5-μm width along each line and plotted against time. Each trace is the average of five records. (B) The initial phases of single impulse-induced rise in $[Ca^{2+}]_i$ are expanded in time to show no change in the peak time after the conditioning tetanus. (C) Changes in $[Ca^{2+}]_i$ produced by individual stimuli of the conditioning tetanus. Only those in the initial and the late (4 min) phases of stimuli are shown. (D) The decay time course of the increased basal $[Ca^{2+}]_i$ after the conditioning tetanus.

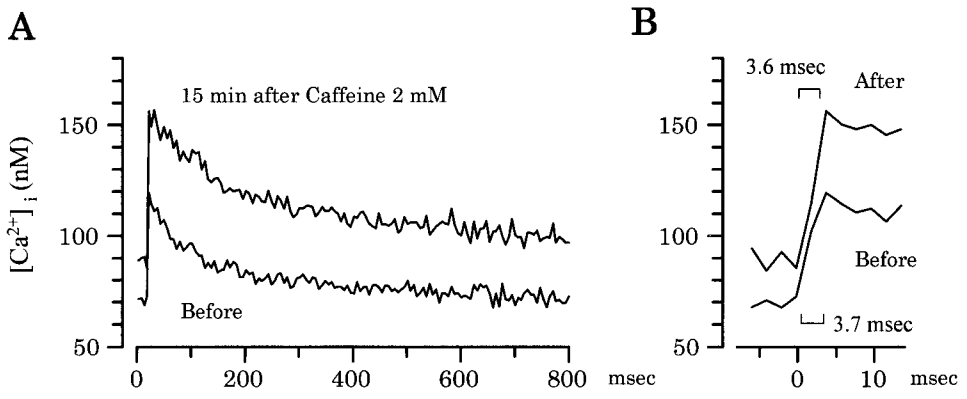

Figure 8. Enhancement of single impulse-induced rises in $[Ca^{2+}]_i$ by caffeine. Single impulse-induced rises in $[Ca^{2+}]_i$ were recorded by line scanning the terminal loaded with dOGB-1 with a confocal microscope in normal Ringer's, and changes in the fluorescence of dOGB-1 were averaged over 3–5-μm width along each line and plotted against time. Each trace is the average of five records. The records are shown in two different time scales (A and B).

The extent of the prolongation, however, was not large, suggesting that CICR occurs in a region close to the Ca^{2+} microdomain produced by Ca^{2+} entry and contributes directly to impulse-induced exocytosis (see discussion).

Enhancement of Transmitter Exocytosis in Parallel with the Extent of the Activation of CICR

How the use-dependent changes of transmitter release are affected by the extent of activation of CICR was examined by observing changes in EPPs and $[Ca^{2+}]_i$ in the terminals in response to repetitive tetani. Effects of combinations of a tetanus of 33.3 or 50 Hz and a period of a low rate stimuli (0.5 or 1 Hz), each for 30 s, were first observed on EPPs in a low Ca^{2+}, high Mg^{2+} solution (Fig. 10 A). The amplitude of EPPs induced by each tetani showed complex patterns of changes during the course of tetani. It is, however, clear in overall that the amplitude of EPPs initially increased (waxing phase), reached the maximum, and then declined with the repetition of tetani (waning phase; Fig. 10 A). Detailed analyses and consideration of changes in EPPs in response to each tetani revealed changes in the activity-dependent modification of transmitter release during the course of a slow priming, subsequent activation, and inactivation of CICR.

Fig. 10 (B and C) shows changes in QC of EPP during and after each repetitive high frequency tetani. QC was monotonously increased during the first and second tetanus (Fig. 10 B). Increases in QC during each subsequent tetani were diphasic; the initial rapid rise and the subsequent slow rise (or decline). The magnitude and rate of the initial growth phase of QC increased with repetition of tetani until the maximum response was reached (in the waxing phase; Fig. 10 B). Then, the magnitude of the initial phase decreased with a slight reduction in rate of rise in the later tetani (in the waning phase; Fig. 10 C). The rate of rise of the second phase during a tetanus was unchanged in the third to fifth tetani and became plateau in the sixth tetanus (Fig. 10 B). The second phase then changed to a declining phase for tetani applied after the maximum response was reached (in the waning phase; Fig. 10 C).

Changes in $[Ca^{2+}]_i$ in the nerve terminal during each repetitive tetani were then observed in experiments separately from those for EPPs. The results were in general similar to those of EPP except for two respects (see below; Fig. 11, A–C). The diphasic rise in $[Ca^{2+}]_i$ was seen in all Ca^{2+} responses. (Its absence in trains of EPPs in the first and second tetanus may be explained by the low probability of transmitter release under this condition.) The declining rate of the second phase of an increased $[Ca^{2+}]_i$ during each tetani in the waning phase was faster than that of QC in the corresponding

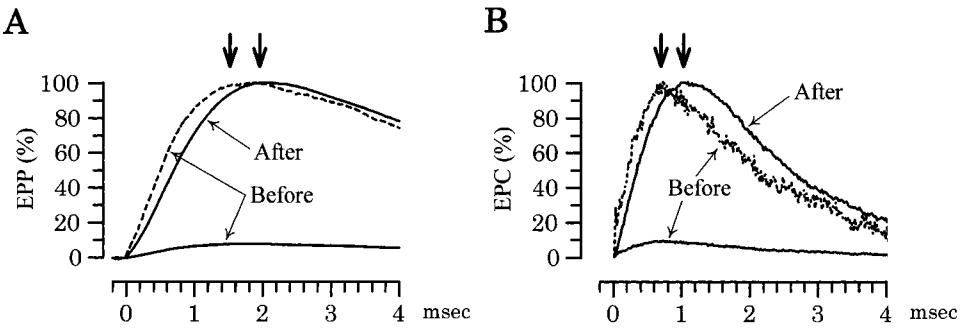

Figure 9. Changes in the time course of EPPs and EPCs after the conditioning tetanus. (A) EPPs before and after a conditioning tetanus. All EPPs in trains recorded before the tetanus were averaged, while the first EPPs in trains after the conditioning tetanus (10 Hz, 10 min) were averaged. The time courses of EPP recorded before the conditioning tetanus are shown in relative (continuous curves) and normalized (dotted curves) magnitudes to those after the tetanus. Arrows indicate the peak of EPP. (B) EPCs before and after a conditioning tetanus. The time course of EPC was calculated by the deconvolution of that of EPP (see materials and methods). Other explanations are the same as those in A.

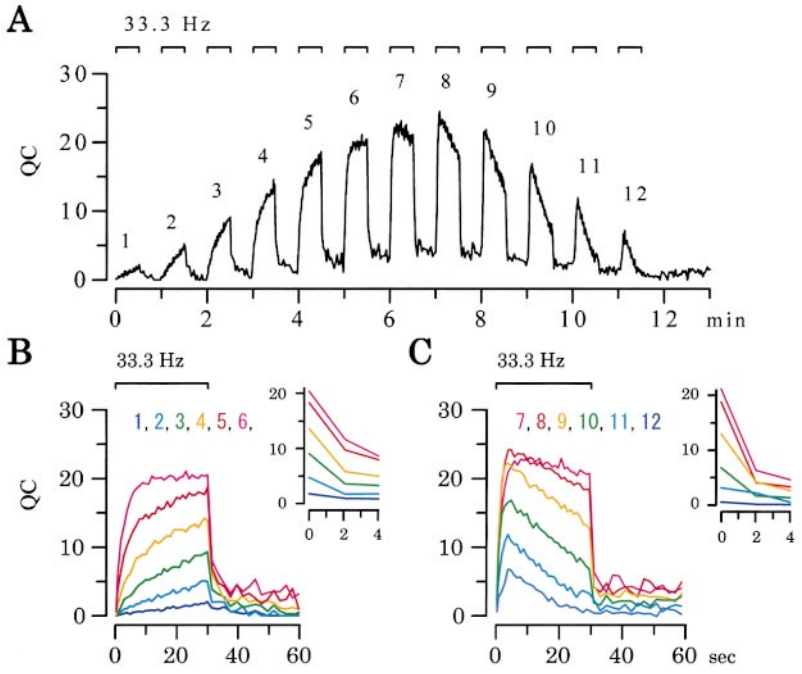

Figure 10. Changes in QC of EPPs induced by a high frequency tetanus during the course of priming and inactivation of the mechanism of CICR. (A) Changes in QC of EPPs induced by repetition of tetani in a low Ca^{2+} (0.5 mM), high Mg^{2+} (10 mM) solution. Combination of a high frequency tetanus (33.3 Hz, 30 s) and low frequency stimuli (0.5 Hz, 30 s) were repeated. QC averaged over those of 20 EPPs throughout all tetani is plotted. (B and C) Changes in QC during and after each high frequency tetani shown in A. Responses to each tetani during the waxing phase of QC are shown in an expanded time scale (B), while those during the waning phase are shown in (C). Insets are the early decay phases of the enhancement of QC after each tetani during the waxing (B) and waning (C) phases.

phase (Fig. 11 C). [Augmentation and potentiation of transmitter release developed during tetanus (see below) could explain the slower decay of QC.] Aside from these differences, similar changes in EPP and $[Ca^{2+}]_i$ in the nerve terminal during repetition of tetani can be accounted for by the priming and inactivation of CICR (Narita et al., 1998). The waxing and waning of the initial phase of increases in EPP and $[Ca^{2+}]_i$ during each tetani reflect the extent of priming and inactivation of CICR, respectively, which modified or produced augmentation and potentiation, while those of the second phase represent the rates of priming and inactivation, respectively, during each tetani.

Enhancement of Augmentation and Potentiation in Parallel with the Extent of CICR Activation

Changes in augmentation and potentiation induced by repetition of tetani are shown by the decay of in-

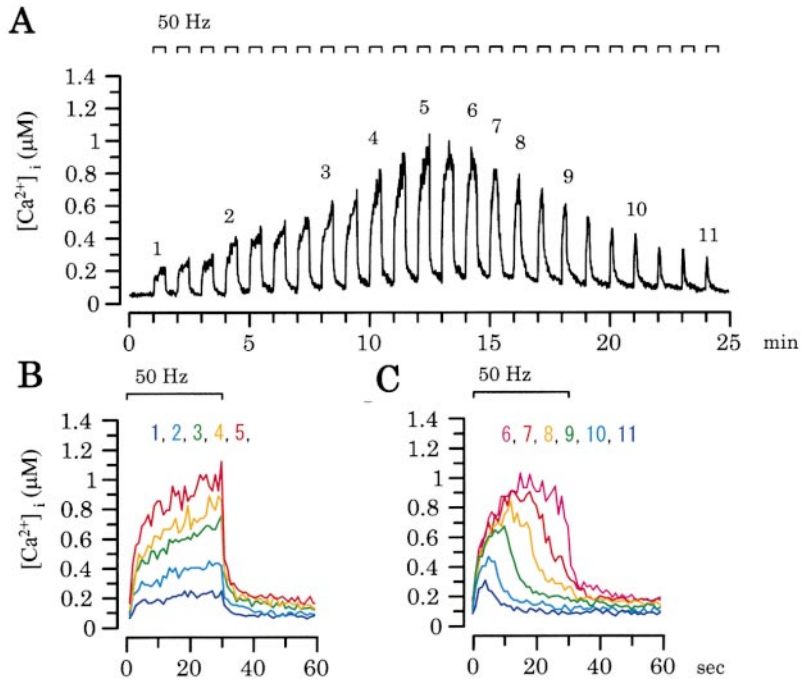

Figure 11. Changes in rises of $[Ca^{2+}]_i$ in response to a high frequency tetanus during the course of priming and inactivation of the mechanism of CICR. (A) Changes in the magnitude of a rise in $[Ca^{2+}]_i$ induced by a high frequency tetanus during repetition of tetani in a low Ca^{2+} (0.5 mM), high Mg^{2+} (10 mM) solution. Combination of a high frequency tetanus (50 Hz, 30 s) and low frequency stimuli (0.5 Hz, 30 s) were repeated, and changes in $[Ca^{2+}]_i$ were measured by recording changes in fluorescence of dOGB-1 loaded in the nerve terminal using an intensified CCD camera. (B and C) Changes in an increase in $[Ca^{2+}]_i$ in response to each high frequency tetani shown in A. Responses to each tetani during the waxing phase of an increased $[Ca^{2+}]_i$ are shown in an expanded time scale (B), while those during the waning phase are shown in C.

creased QC of EPPs (induced at 0.5 or 1 Hz) after each tetani. The enhancement of QC declined in two phases with time constants of about a few and several tens of seconds (the precise measurement was not possible for the sparse time resolution; Fig. 10, B and C, insets). The initial fast phase would represent the decay of augmentation. The second slow phase, which was almost sustained as repetition of tetani proceeded, could be due to the decay of potentiation (Magleby and Zengel, 1975; Zengel and Magleby, 1982) and the depriming of CICR, as shown in Fig. 4 A. The magnitudes of these components of QC were increased in the waxing phase of responses during repetition of tetani (Fig. 10 B), and then decreased in the waning phase (Fig. 10 C). The increases of these components of QC in the waxing phase indicate the enhancement of augmentation and potentiation in parallel with the growth of CICR activation, while the decreases in the waning phase may reflect the reduction of augmentation, potentiation, and CICR. The decrease in the second slow component of the increased QC with repetition of tetani in the waning phase (Fig. 10 C), however, was slightly faster than the late decay component of the enhanced EPP after a long conditioning tetanus (Fig. 4 A). Such a faster decrease may also involve other factors, such as depletion of transmitter pool, although it is not large and is equivalent to that caused by stimulation at 3.3 Hz in normal Ringer (33.3 Hz $\times$ 20 QC = 3.3 Hz $\times$ 200 QC).

DISCUSSION

The present study demonstrates that the conditioning tetanus to the nerve for priming the mechanism of CICR produced the marked enhancement of the amplitude and QC of end-plate potentials, which was blocked by inhibitors of ryanodine receptors. The enhancement decayed in two phases with the time constants of 1.85 and 10 min, which correspond to those of the use-dependent potentiation of transmitter release and the depriming rate of CICR, respectively, and accompanied by a slight prolongation of the peak times of EPP and EPC. The conditioning nerve stimulation also enhanced single impulse- and tetanus-induced rises in intracellular Ca^{2+} in the terminals with little change in time course. Facilitation of EPPs induced by a short train was not changed after the conditioning stimulation, while augmentation and potentiation of EPP induced by a high frequency long tetanus were enhanced by repetition of long tetani that slowly primed CICR. It is discussed below how these results support the hypothesis that ryanodine receptors exist close to voltage-gated Ca^{2+} channels in the presynaptic terminals and amplify the impulse-evoked exocytosis and its plasticity via CICR after the Ca^{2+}-dependent priming.

Impulse-induced Ca^{2+} Dynamics in the Active Zone and Global Cytoplasm

It may be necessary to review briefly the current understanding of impulse-induced Ca^{2+} dynamics in presynaptic nerve terminals as the basis of interpreting the present findings in terms of the roles of CICR in the exocytosis of transmitter and its short-term plasticity. Ca^{2+} entry through voltage-dependent Ca^{2+} channels activated by a nerve impulse increases $[Ca^{2+}]_i$ to >100 μM at the active zone and activates exocytosis of transmitter (Katz, 1969; Llinás et al., 1992; Heidelberger et al., 1994; Schweitzer et al., 1995). Ca^{2+} ions in the high $[Ca^{2+}]_i$ domain spread throughout the cytoplasm by diffusion, while they are being bound to Ca^{2+}-binding proteins or taken up into organelles (Sala and Hernández-Cruz, 1990; Sinha et al., 1997). Thus, most of the increased $[Ca^{2+}]_i$ decays within a few milliseconds and the residual component disappears with a time constant of tens of milliseconds (Simon and Llinás, 1985; Digregorio et al., 1999; Suzuki et al., 2000). Because of the extremely short lifetime of the high $[Ca^{2+}]_i$ and its fast binding and unbinding to the Ca^{2+}-binding proteins of low affinity for the exocytotic machinery, the process of impulse-induced exocytosis is most resistant to the action of fast chelator, BAPTA, among Ca^{2+}-dependent presynaptic processes (Tanabe and Kijima, 1992) and unaffected by a slow chelator, EGTA. On the other hand, the $[Ca^{2+}]_i$ in the global cytoplasm rises to a moderate level with a slower rate and cleared by several independent mechanisms with time constants of tens of milliseconds, hundreds of milliseconds, and several seconds (Suzuki et al., 2000). The decay time courses of these residual $[Ca^{2+}]_i$ in the active zone and global cytoplasm cause various forms of short-term plasticity, fast (time constant, 30–60 ms) and slow (200–400 ms) facilitation, augmentation (several seconds), and potentiation (several tens of seconds).

No Apparent Changes in Facilitation by the Activation of CICR

The high level of residual Ca^{2+} in the microdomain would produce the fast component of facilitation via the Ca^{2+}-sensing protein for the exocytotic machinery (Katz and Miledi, 1968) or a similar one (Kamiya and Zucker, 1994; Delaney and Tank, 1994), as supported by the following evidence. Fast facilitation is similar in decay time constant to the decay time course of the $[Ca^{2+}]_i$ in the microdomain estimated in simulation (Suzuki et al., 2000). Fast facilitation is reported to be most effectively blocked by loading BAPTA (Tanabe and Kijima, 1989), but less by EGTA (Suzuki et al., 2000) or uncaging chelators in presynaptic terminals (Kamiya and Zucker, 1994), as expected from the involvement of a low-affinity Ca^{2+} binding protein and the short life time of the high residual $[Ca^{2+}]_i$. Furthermore, the residual $[Ca^{2+}]_i$ less than micromolar in the

global cytoplasm cannot explain fast facilitation produced via the low affinity Ca^{2+} receptor ($\sim$100 μM; see Suzuki et al., 2000).

In the present experiments, fast facilitation of transmitter release produced by a short train of stimuli was not changed after a conditioning tetanus that primes the mechanism of CICR. Since fast facilitation is highly likely caused by the residual $[Ca^{2+}]_i$ in the microdomain after a nerve impulse (see above), this absence of the effect of CICR activation on facilitation could be accounted for by two possibilities. First, CICR would occur in a region remote from the active zones so that it does not affect facilitation. In this case, CICR does not directly enhance the impulse-induced exocytosis of transmitter. Second, CICR may amplify the residual $[Ca^{2+}]_i$ in the Ca^{2+} microdomain for exocytosis in proportion to the enhancement of the impulse-induced increase in $[Ca^{2+}]_i$ there. (This mode of increases in the residual $[Ca^{2+}]_i$ in the microdomain may not be held, however, in normal Ringer solution for the nonlinear binding of Ca^{2+} to buffers in the terminal.) This implies that CICR takes place in the Ca^{2+} microdomain for exocytosis so that CICR would directly activate the Ca^{2+}-sensing protein for the exocytotic machinery (see below).

Since the slow component of facilitation was not separated from changes in the amplitude of EPPs induced by a short train, it was not studied how CICR affects this component. It may be possible that slow facilitation could be affected by CICR, similar to augmentation and potentiation for its similar Ca^{2+} dependence (see below).

Enhancement of Augmentation and Potentiation by the Activation of CICR

The moderate level of residual Ca^{2+} in the global cytoplasm (and also the microdomain) would activate (or enhance) the mechanisms of slow facilitation (Suzuki et al., 2000; see also Tanabe and Kijima, 1992), augmentation, and potentiation (Kamiya and Zucker, 1994; Delaney and Tank, 1994; Regehr et al., 1994) via a high-affinity Ca^{2+} receptor. The time courses of augmentation and potentiation (and presumably also slow facilitation) therefore follow the time course of the global rise in $[Ca^{2+}]_i$ in the terminal, although augmentation and potentiation would remain longer than the increased $[Ca^{2+}]_i$ for their longer lifetime of activation (Regehr et al., 1994). The involvement of high-affinity Ca^{2+} binding proteins of rather slow binding and unbinding rates in augmentation and potentiation can be suggested by the following observations. Tanabe and Kijima (1989, 1992) showed little effect of BAPTA on slow facilitation, augmentation, and potentiation at frog motor nerve terminals, while EGTA weakly affected slow facilitation (Suzuki et al., 2000). The rather slow rate (relative to that on fast facilitation) of the appearance of the blocking action of uncaged chelators on augmentation and potentiation was seen at crayfish motor nerve terminals (Kamiya and Zucker, 1994).

In the present study, repetition of tetani demonstrated that augmentation and potentiation were enhanced in parallel with the increase in the magnitude of CICR by the priming of CICR. In addition, the initial decay time constant (1.85 min; Fig. 4 A) of enhancement of EPP after a long conditioning tetanus that primed CICR was similar to the decay time constant of a rise in $[Ca^{2+}]_i$ induced by a similar conditioning tetanus (1.65 min; Fig. 7 D), and also similar to the time constant calculated from the experimentally derived equation for the decay of potentiation (Magleby and Zengel, 1975). This conforms to the role of the residual $[Ca^{2+}]_i$ in the global cytoplasm in potentiation (Delaney and Tank, 1994; Kamiya and Zucker, 1994; Regehr et al., 1994; see above). Furthermore, potentiation of transmitter release by a long conditioning tetanus was completely blocked by ryanodine (Fig. 4). Although it remains to be studied whether the activation of CICR is fully essential for the generation of potentiation, it is quite clear that the largest fraction of potentiation depends on the rise in $[Ca^{2+}]_i$ caused by the activation of CICR. This is consistent with the inhibition of potentiation by caffeine (Onodera, 1973) and more or less similar to the role of Ca^{2+} release in potentiation at other terminals, albeit the origins and/or pathways for Ca^{2+} release are different (Hashimoto et al., 1996; Tang and Zucker, 1997).

Involvement of CICR in the Impulse-induced Exocytosis of Transmitter

The question as to whether or not CICR occurs in the Ca^{2+} microdomains for exocytosis can be examined by analyzing the temporal characteristics of single impulse-induced rise in $[Ca^{2+}]_i$. The impulse-induced rise in $[Ca^{2+}]_i$ involving CICR should be the algebraic sum of the time course of the rises in $[Ca^{2+}]_i$ produced by Ca^{2+} entry and CICR. These processes could be obviously hampered to some extent by the rate of Ca^{2+} binding to Ca^{2+}-binding proteins and Ca^{2+} probes (Sala and Hernández-Cruz, 1990; Sinha et al., 1997), the saturation of Ca^{2+} probes and the nonlinear dependence of the global $[Ca^{2+}]_i$ on the domain $[Ca^{2+}]_i$. Nevertheless, the activation of CICR should be delayed to a Ca^{2+} entry-induced rise in $[Ca^{2+}]_i$ for the time of Ca^{2+} diffusion from the site of Ca^{2+} entry to the site of CICR and the rate of the resultant Ca^{2+} release. This time delay would thus be reflected in the time course of the impulse-induced rise in $[Ca^{2+}]_i$, depending on Ca^{2+} diffusion path. If CICR occurs at a site close to the site of Ca^{2+} entry in the active zone, a single impulse-induced increase in $[Ca^{2+}]_i$ would rise monophasically with or without slight prolongation of the peak time. If CICR occurs at a site remote enough from that of Ca^{2+}

entry, the time delay for the activation of CICR should be considerably greater and result in diphasic or show double peaks of single impulse-induced rise in $[Ca^{2+}]_i$ or at least its prolongation.

There was no change in the peak time of the single impulse-induced rise in $[Ca^{2+}]_i$ that was enhanced by a conditioning tetanus (Fig. 7 B). Thus, CICR should occur within the time resolution of 2 ms for $[Ca^{2+}]_i$ measurement. Furthermore, if the peak time of the rate of rises in impulse-induced fluorescence is measured with a low affinity Ca^{2+} indicator (Sabatini and Regehr, 1998), this upper bound of 2 ms for the latency of CICR could be much smaller.

The time difference between Ca^{2+} entry and the resultant Ca^{2+} release was more relevantly measured by the analysis of the rising phase of EPC, which would reflect the rate of rise of transmitter release and, therefore, that of transmitter exocytosis. The peak time of EPC was increased by 200 μs (Fig. 9 B) after a conditioning tetanus. This prolongation of the time course of impulse-induced exocytosis could reflect the prolongation of the life time of the high $[Ca^{2+}]_i$ in the active zone involved in exocytosis. [It is unlikely that the prolongation results from the increased life time of transmitter in the synaptic cleft by the conditioning tetanus (e.g., by inhibiting cholinesterase), since it is unrealistic to assume that presynaptic nerve activity inhibits the enzyme.] The prolongation of the rising phase of EPC together with the enhancements of impulse-induced rise in $[Ca^{2+}]_i$ and exocytosis thus suggest the recruitment of additional trigger Ca^{2+} for exocytosis, which is CICR. In other words, the results strongly indicate the activation of CICR in, or in a region close to, the active zone. The upper bound for the distance (r) between a Ca^{2+} channel and a ryanodine receptor for Ca^{2+} diffusion may be estimated from the increase in the peak time (200 μs) of EPC and found to be <109 nm [$r = (6\ tD)^{1/2} = 109$ nm: D, diffusion coefficient, 10^{-7} cm^2/s; Regehr and Atluri, 1995].

There are other lines of evidence for the occurrence of CICR in the active zone of the motor nerve terminals. First, the late decay component of the enhancement of EPPs after a conditioning tetanus slower than that of potentiation must be explained by a new mechanism. The time constant (10.4 min) of this slower decay component of EPP enhancement (Fig. 4 A) is similar to the decay time course of the increase in the single or repetitive impulse(s)-induced rise in $[Ca^{2+}]_i$ after a conditioning tetanus (Figs. 5 and 7) and also to that of the depriming process of CICR (Narita et al., 1998). Second, the mechanism of CICR remained to be inactivated by repetitive Ca^{2+} entries with a negligibly small elevation of the basal $[Ca^{2+}]_i$ in a low Ca^{2+}, high Mg^{2+} solution, but was quickly restored from inactivation by stopping Ca^{2+} entry for a few seconds (Narita et al., 1998). This finding indicates the inactivation of ryanodine receptor (Sutko and Airey, 1996) by a rise in $[Ca^{2+}]_i$ close to the site of Ca^{2+} entry, and also the activation of CICR in the active zone.

Consequently, it is highly likely that CICR occurs at a site close to the high $[Ca^{2+}]_i$ microdomain produced by a nerve impulse and is directly involved in the impulse-induced exocytosis of transmitter. The absence of changes in facilitation of transmitter release during the enhancement of impulse-induced exocytosis then suggests that the impulse-induced rise in $[Ca^{2+}]_i$ at the active zone and the residual $[Ca^{2+}]_i$ there are proportionally amplified by the activation of CICR (see above). Furthermore, the augmentation and potentiation of EPP induced by a relatively long tetanus in frog motor nerve terminals was little affected by BAPTA (Tanabe and Kijima, 1989). This observation could be explained by the occurrence of CICR in the active zone and its enhancement (or activation) of augmentation and potentiation.

The magnitude of the enhancement of exocytosis that attributed to an increase in $[Ca^{2+}]_i$ by CICR at the exocytotic sites may be estimated from the fraction of the later decay phase of the enhancement of EPP by a conditioning tetanus. It was 51% of the total enhancement at the end of the tetanus (Fig. 4). The amplification (or generation) of augmentation and potentiation by CICR can explain other components of the enhancement.

Physiological Significance of the Unique CICR Mechanism at Presynaptic Terminals

The physiological significance of the marked enhancement of evoked exocytosis by the unique CICR mechanism at the frog motor nerve terminals lies in its novel mechanisms of priming and activation. The mechanism of priming of CICR is now being studied (Hachisuka et al., 1999). It is at least known that the priming process depends on the rate of nerve stimulation and external Ca^{2+}, indicating the amount of Ca^{2+} entry (Narita et al., 1998). The loading of Ca^{2+} into Ca^{2+} stores in the terminals does not appear to be the mechanism for the priming process (particularly in a low Ca^{2+}, high Mg^{2+} solution), as already discussed in the previous study (Narita et al., 1998). In brief, the slow rising phase of the conditioning tetanus-induced increase in $[Ca^{2+}]_i$ must be caused by Ca^{2+} entry at the cell membrane and CICR through slowly primed ryanodine receptors. The fraction of the former was found to be much smaller than that of the latter, as evidenced by a small tetanus-induced rise in $[Ca^{2+}]_i$ in the presence of a blocker of ryanodine receptors in a low Ca^{2+}, high Mg^{2+} solution (see Figure 3 of Narita et al., 1998). Accordingly, CICR would play a major role in the conditioning tetanus-induced increase in $[Ca^{2+}]_i$, indicating Ca^{2+} efflux across the Ca^{2+} store membranes under this condition (Narita et al., 1998). The priming effect of caffeine on CICR without a conditioning stimulation

in both normal (Fig. 8) and low Ca^{2+}, high Mg^{2+} solutions (our unpublished observations) also rules out the role of Ca^{2+} loading into Ca^{2+} stores in the priming process during a conditioning tetanus.

This new, use-dependent mode of modification of transmitter exocytosis is now added to, and/or provides in part a mechanism for some of the well-known short-term plasticity. For a short train of presynaptic nerve activity (e.g., less than tens of impulses) facilitation would play a major role in use-dependent plasticity. Longer lasting activity for more than several seconds significantly produces a global rise in $[Ca^{2+}]_i$ in the presynaptic terminals and activates augmentation and potentiation, some, if not all, of which could be boosted by the partial activation of CICR. Much longer lasting activity fully primes the mechanism of CICR and produces the marked enhancement of transmitter release by several tens of times, which lasts for >10 min, until the mechanism of CICR is deprimed. The use-dependent efficacy of impulse-induced exocytosis may thus be expressed by the modification of the multiplicative equation comprising each component of the known short-term plasticity (Magleby and Zengel, 1982; Tanabe and Kijima 1992) with the addition of the new component involving CICR.

$$\text{Efficacy} = (F_1 + 1)(F_2 + 2)(A + 1)(P + 1)(R + 1),$$

where F_1, F_2, A, P, and R are the fraction of increases produced by fast and slow facilitation, augmentation, potentiation, and CICR, respectively. As already indicated, the increases in $[Ca^{2+}]_i$ involved in augmentation and potentiation, especially the latter, are strongly amplified by the activation of CICR at the frog motor nerve terminals.

This unique priming-dependent activation of CICR and its strong facilitatory effects on transmitter release provides in general the important mechanism for the plasticity of synaptic gain. In fact, a similar enhancement of transmitter exocytosis was seen in nicotinic synapses of bullfrog sympathetic ganglia (Takeuchi et al., 1999). If this mechanism exists in central synapses, it could be the basis for the mechanisms of short-term memory and learning. Furthermore, it may settle the controversy over the extent of involvement of CICR in synaptically induced rises in $[Ca^{2+}]_i$ in the spines and dendrites of central neurons (Svoboda and Mainen, 1999), if the CICR there has a priming process.

We thank Prof. H. Kijima for critical comments to the earlier version of the manuscript and Dr. T. Takai for kind computation of EPC.

This study was supported in part by Grants in Aid for Scientific Research (K. Kuba) from the Japanese Ministry of Education, Science and Culture and a Research Project Grant (K. Narita) from Kawasaki Medical School.

Submitted: 13 December 1999
Revised: 28 February 2000
Accepted: 29 February 2000

REFERENCES

Chiou, C.Y., and M.H. Malagodi. 1975. Studies on the mechanism of action of a new Ca^{2+} antagonist, 8-(*N*,*N*-diethylamino) octyl 3,4,5-trimethoxybenzoate hydrochloride in smooth and skeletal muscles. *Brit. J. Pharmacol.* 53:279–285.

David, G., J.N. Barrett, and E.F. Barrett. 1997. Stimulation-induced changes in $[Ca^{2+}]_i$ in lizard motor nerve terminals. *J. Physiol.* 504: 83–96.

Delaney, K.R., and D.W.A. Tank. 1994. Quantitative measurement of the dependence of short-term synaptic enhancement on presynaptic residual calcium. *J. Neurosci.* 14:5885–5902.

DiGregorio, D.A., and J.L. Vergara. 1997. Localized detection of action potential-induced presynaptic calcium transients at a *Xenopus* neuromuscular junction. *J. Physiol.* 505:585–592.

DiGregorio, D.A., A. Peskoff, and J.L. Vergara. 1999. Measurement of action potential-induced presynaptic calcium domains at a cultured neuromuscular junction. *J. Neurosci.* 15:7846–7859.

Fatt, P., and B. Katz. 1951. An analysis of the end-plate potential recorded with an intracellular electrode. *J. Physiol.* 115:320–370.

Finch, E.A., and G.J. Augustine. 1998. Local calcium signalling by inositol-1,4,5,-trisphosphate in Purkinje cell dendrites. *Nature.* 396:753–756.

Friel, D.D., and R.W. Tsien. 1992. A caffeine- and ryanodine-sensitive Ca^{2+} store in bullfrog sympathetic neurons modulates the effects of Ca^{2+} entry on $[Ca^{2+}]_i$. *J. Physiol.* 450:217–246.

Gage, P.W. 1976. Generation of end-plate potentials. *Physiol. Rev.* 56:177–247.

Gage, P.W., and R.N. McBurney. 1973. An analysis of the relationship between the current and potential generated by a quantum of acetylcholine in muscle fibers without transverse tubules. *J. Membr. Biol.* 12:247–272.

Garaschuk, O., Y. Yaari, and A. Konnerth. 1997. Release and sequestration of calcium by ryanodine-sensitive stores in rat hippocampal neurones. *J. Physiol.* 502:13–30.

Hachisuka, J., T. Akita, K. Narita, H. Kijima, and K. Kuba. 1999. Characteristics of the priming process of Ca^{2+}-induced Ca^{2+} release at frog motor nerve terminals. *Soc. Neurosci. Abstr.* 25:1252.

Hashimoto, T., T. Ishii, and H. Ohmori. 1996. Release of Ca^{2+} is the crucial step for the potentiation of IPSCs in the cultured cerebellar Purkinje cells of the rat. *J. Physiol.* 497:611–627.

Heidelberger, R., C. Heinemann, E. Neher, and G. Matthews. 1994. Calcium dependence of the rate of exocytosis in a synaptic terminal. *Nature.* 371:513–515.

Hua, S.-Y., M. Nohmi, and K. Kuba. 1993. Characteristics of Ca^{2+} release induced by Ca^{2+} influx in cultured bullfrog sympathetic neurones. *J. Physiol.* 464:245–272.

Kamiya, H., and R.S. Zucker. 1994. Residual Ca^{2+} and short-term synaptic plasticity. *Nature.* 371:603–606.

Katz, B. 1969. The release of neural transmitter substances. Charles C. Thomas. Springfield, IL. 33–39.

Katz, B., and R. Miledi. 1968. The role of calcium in neuromuscular facilitation. *J. Physiol.* 195:481–492.

Kuba, K. 1980. Release of calcium ions linked to the activation of potassium conductance in a caffeine-treated sympathetic neurone. *J. Physiol.* 298:251–269.

Kuba, K. 1994. Ca^{2+}-induced Ca^{2+} release in neurones. *Jpn. J. Physiol.* 44:613–650.

Llano, I., R. Dipolo, and A. Marty. 1994. Calcium-induced calcium release in cerebellar Purkinje cells. *Neuron.* 12:663–673.

Llinás, R., M. Sugimori, and R.B. Silver. 1992. Microdomains of high calcium concentration at a presynaptic terminal. *Science.* 256:677–679.

Magleby, K.L., and J.E. Zengel. 1975. A dual effect of repetitive stimulation on post-tetanic potentiation of transmitter release at the frog neuromuscular junction. *J. Physiol.* 245:163–182.

Magleby, K.L., and J.E. Zengel. 1982. A quantitative description of stimulation-induced changes in transmitter release at the frog neuromuscular junction. *J. Gen. Physiol.* 80:613–618.

Mothét, J.-P., P. Fossier, F.-M. Meunier, J. Sinnakre, L. Tauc, and G. Baux. 1998. Cyclic ADP-ribose and calcium-induced calcium release regulate neurotransmitter release at a cholinergic synapse of *Aplysia*. *J. Physiol.* 507:405–414.

Narita, K., T. Akita, M. Osanai, T. Shirasaki, H. Kijima, and K. Kuba. 1998. A Ca^{2+}-induced Ca^{2+} release mechanism involved in asynchronous exocytosis at frog motor nerve terminals. *J. Gen. Physiol.* 112:593–609.

Onodera, K. 1973. Effect of caffeine on the neuromuscular junction of the frog, and its relation to external calcium concentration. *Jpn. J. Physiol.* 23:587–597.

Regehr, W.G., and P.P. Atluri. 1995. Calcium transients in cerebellar granule cell presynaptic terminals. *Biophys. J.* 68:2156–2170.

Regehr, W.G., K.R. Delaney, and D.W. Tank. 1994. The role of presynaptic calcium in short-term enhancement at the hippocampal mossy fiber synapse. *J. Neurosci.* 14:523–537.

Sabatini, B.L., and W.G. Regehr. 1998. Optical measurement of presynaptic calcium currents. *Biophys. J.* 74:1549–1563.

Sala, F., and A. Hernández-Cruz. 1990. Calcium diffusion modeling in a spherical neuron. Relevance of buffering properties. *Biophys. J.* 57:313–324.

Schweitzer, F.E., H. Betz, and A.G. Augustine. 1995. From vesicle docking to endocytosis: intermediate reactions of exocytosis. *Neuron*. 14:689–696.

Simon, S.M., and R.R. Llinás. 1985. Compartmentalization of the submembrane calcium activity during calcium influx and its significance in transmitter release. *Biophys. J.* 48:485–498.

Sinha, S.R., L.G. Wu, and P. Saggau. 1997. Presynaptic calcium dynamics and transmitter release evoked by single action potentials at mammalian central synapses. *Biophys. J.* 72:637–651.

Smith, A.B., and T.C. Cunnane. 1996. Ryanodine-sensitive calcium stores involved in neurotransmitter release from sympathetic nerve terminals of the guinea-pig. *J. Physiol.* 497:657–664.

Sutko, J.L., and J.A. Airey. 1996. Ryanodine receptor Ca^{2+} release channels: does diversity in form equal diversity in function? *Physiol. Rev.* 76:1027–1071.

Suzuki, S., M. Osanai, M. Murase, N. Suzuki, K. Ito, T. Shirasaki, K. Narita, K. Ohnuma, K. Kuba, and H. Kijima. 2000. Ca^{2+} dynamics at the frog motor nerve terminal. *Pflügers Arch*. In press.

Svoboda, K., and Z.F. Mainen. 1999. Synaptic [Ca^{2+}]: Intracellular stores spill their guts. *Neuron*. 22:427–430.

Takechi, H., J. Eilers, and A. Konnerth. 1998. A new class of synaptic response involving calcium release in dendritic spines. *Nature*. 396:757–760.

Takeuchi, A., and N. Takeuchi. 1959. Active phase of frog's endplate potential. *J. Neurophysiol.* 22:395–411.

Takeuchi, S., H. Tokuno, A. Nishi, and K. Kuba. 1999. Involvement of intracellular Ca^{2+} release in use-dependent potentiation of transmitter release at nicotinic synapses of bullfrog sympathetic ganglia. *Soc. Neurosci. Abstr.* 25:1253.

Tanabe, N., and H. Kijima. 1992. Ca^{2+}-dependent and -independent components of transmitter release at the frog neuromuscular junction. *J. Physiol.* 455:271–289.

Tanabe, N., and H. Kijima. 1989. Both augmentation and potentiation occur independently of internal Ca^{2+} at the frog neuromuscular junction. *Neurosci. Lett.* 99:147–152.

Tang, Y.-Q., and R.S. Zucker. 1997. Mitochondrial involvement in post-tetanic potentiation of synaptic transmission. *Neuron*. 18: 483–491.

Zengel, J.E., and K.L. Magleby. 1982. Augmentation and facilitation of transmitter release. A quantitative description at the frog neuromuscular junction. *J. Gen. Physiol.* 80:583–611.

Zucker, R.S. 1996. Exocytosis: a molecular and physiological perspective. *Neuron*. 17:1049–1055.